JOURNAL OF MATERIALS SCIENCE **36** (2001) 2335–2342

Effect of crosshead speed on the fracture toughness of Soda-lime glass, Al_2O_3 and Si_3N_4 ceramics determined by the surface crack in flexure (SCF) method

JONG-KEUK PARK
Now with research Institute of Advanced Materials, Seoul National University, Seoul 151-742, Korea
E-mail: jokepark@snu.ac.kr

KOUICHI YASUDA, YOHTARO MATSUO
Department of Metallurgy and Ceramics Science, Tokyo Institute of Technology 2-12-1 Ookayama, Meguro-ku, Tokyo 152-8552, Japan

The fracture toughness of soda-lime glass, Al_2O_3 and Si_3N_4 specimens was measured by the surface crack in flexure method. For the soda-lime glass specimens, the fracture toughness was calculated from the initial crack size and flexure strength, and the value increased with increasing crosshead speed. This trend seems to be related to the difficulty in determining the critical crack size at fracture, since slow crack growth occurs during bending test. For the Al_2O_3 specimens, a halo region (stable crack growth region) was formed around the initial precrack during bending test. The halo size increased and the resultant flexure strength decreased with decreasing in the crosshead speed. The halo region, however, could not be observed in the Si_3N_4 specimens. Despite of the difference in the appearance of halo region, the fracture toughness of the Al_2O_3 and Si_3N_4 specimens was constant irrespective of the crosshead speed when the values were calculated with the critical crack sizes at fracture (halo incorporated crack sizes). The constant fracture toughness with the crosshead speed could be explained by the relation between the changes of halo size (thus critical crack size at fracture) and resultant flexure strength.

1. Introduction

The controlled surface flaw (CSF) method was developed in 1970's as a test method for fracture toughness with a small precrack introduced by Knoop or Vickers indentations [1, 2]. Petrovic *et al*. showed that the fracture toughness was affected by the residual stress around the indentation, and refined the method by incorporating the grinding procedure of the indented surface by a certain amount [3, 4]. The method can be described as follows. A small crack is introduced by Knoop or Vickers indentation on a surface of a specimen and the residual stress around the indentation is eliminated by grinding and/or polishing. Then a bending test is conducted to measure the flexure strength of the precracked specimen. The fracture toughness can be estimated from precrack sizes observed on the fractured surface, and the flexure strength using a stress intensity formula as shown in Equation 1.

$$K_{IC} = Y(a, c)\sigma_f \sqrt{a} \tag{1}$$

where Y is the stress intensity shape factor, and σ_f the flexure strength of the precracked specimen, and $2c$ the crack width and a the crack depth. The two Y values for the deepest point of the precrack and the point at surface of the precrack are calculated from the empirical equation of Newman and Raju [5], and the larger Y value is used to calculate the fracture toughness.

It is difficult, however, to measure the precrack size accurately on the fractured surface. Recently, the surface crack in flexure (SCF) method was developed by Quinn *et al*. to improve the CSF method [6–9], and was proposed as an ISO standard for fracture toughness test method [10], after research had been conducted through the round robin project [7, 11]. The mainly refined technique of the SCF method is that the specimen is tilted $\sim 0.5^\circ$ off perpendicular to the diamond indenter axis during the Knoop indentation. By this procedure, the resulting precrack will be 0–5° off normal, and thus tilt slightly from the final fractured surface. This makes the precrack easier to discern during measurement of precrack sizes.

It was reported, however, by Quinn *et al*. that a crack growth region from the initial precrack, which was called as "halo" region, was observed during the bending test by several reasons [9]. In Al_2O_3 and glass

ceramic specimens, for example, the crack growth was caused by slow crack growth (SCG), whereas the crack growth of MgF_2 and AIN specimens was due to the residual stress and crack reorientation, respectively. It is well known that the flexure strength is affected by the crosshead speed during a bending test due to SCG, and thus the crosshead speed for determining flexure strength of ceramics has already been standardized as 0.5 mm/min [12]. It is not clear, however, whether the change in halo size has an influence on the fracture toughness measured by the SCF method or not.

In this study, therefore, the effect of crack growth during a bending test on the fracture toughness was examined using soda-lime glass, Al_2O_3 and Si_3N_4 specimens. In these materials, soda-lime glass and Al_2O_3 specimens were known to show SCG [8, 9, 13–15], whereas Si_3N_4 specimen was not at room temperatures [8]. To change the halo size, the bending test was performed in air by changing the crosshead speed. The effect of 0.5° tilt of the specimen during Knoop indentation was also investigated for the Al_2O_3 specimens.

2. Experimental procedure

High purity Al_2O_3 powder (Taimei Kagaku, TM-D, 99.99%) was hot-pressed at 1400°C for 1 h under 30 MPa in Ar to fabricate Al_2O_3 plates. Si_3N_4 powder mixed with 5 wt%Al_2O_3 and 5 wt%Y_2O_3 (UBE-SN-COA) was also hot-pressed at 1750°C for 1 h under 30 MPa in N_2 to make Si_3N_4 plates. These plates were ground with 200-grit diamond wheel and cut into the rectangular specimens (3 mm × 4 mm × 40 mm). The specimens were annealed at 1400°C for 1 h in air for Al_2O_3 and in N_2 for Si_3N_4 to remove grinding damage. 4 mm wide face of each specimen was polished with 2–4 μm diamond slurry. For the soda-lime glass specimen, the rectangular specimens (2.8 mm × 4 mm × 40 mm) were obtained directly from cutting as-received glass plates.

The 4 mm wide face of each specimen was indented with a Knoop indenter to create a precrack on the surface of the specimen. During the indentation, the specimen was tilted ∼0.5° off perpendicular to the diamond indenter axis. Indentation loads were 37 N for the soda-lime glass specimen, 49 N for Al_2O_3 and Si_3N_4 specimens, respectively. In order to check the influence of tilting a specimen during indentation, some Al_2O_3 specimens were indented without tilting. Some amount of material of the indented surface was removed by polishing to eliminate the residual stress around a Knoop indent. The flexure strength of the indented specimen was measured by a four-point bending fixture (upper span = 10 mm, lower span = 30 mm) under the ambient laboratory conditions (temperature from 25°C to 30°C and relative humidity ∼50%). The crosshead speed was changed from 0.01 mm/min to 5.0 mm/min in order to check the effect of slow crack growth on the fracture toughness. After the bending test, the fractured surfaces were fractographically examined with an optical microscope and a scanning electron microscope (SEM) to determine the initial precrack size and the critical crack size at fracture. The depth (a) and width ($2c$) of the initial precrack size and the critical crack size at fracture were determined from the photographs. The fracture toughness was determined from the flexure strength and these two crack sizes by using the Equation 1.

3. Results and discussion

3.1. Characterization of the specimens

The commercial soda-lime glass plates (Asahi Glass Co.) were used in this study. The chemical composition of the glass was known to be 72.5wt%SiO_2-10.5wt% Na_2O-8.3 wt% CaO-4.1 wt% MgO-2.2 wt% Al_2O_3-0.8 wt% K_2O.

The microstructure of the Al_2O_3 specimen was shown in Fig. 1a. The average grain size of the Al_2O_3 specimen was measured to be around 2.3 μm by the linear intercept method. The crystalline phase was confirmed to be α-Al_2O_3 by X-ray diffraction analysis. The relative bulk density of the Al_2O_3 specimens was larger than 99%.

The main phase of Si_3N_4 grains was confirmed to be β-Si_3N_4 by X-ray diffraction analysis. Fig. 1b shows the microstructure of the Si_3N_4 specimen. The elongated grain structure can be seen in this figure. The average width and average aspect ratio of the elongated grains were determined to be 0.4 μm and 3.8, respectively. The relative bulk density of the Si_3N_4 specimens was about 98.7%.

3.2. Dependence of fracture toughness on crosshead speed

3.2.1. Soda-lime glass specimen

Fig. 2 shows the optical photographs of the fractured surfaces of soda-lime glass specimens. Initial precracks

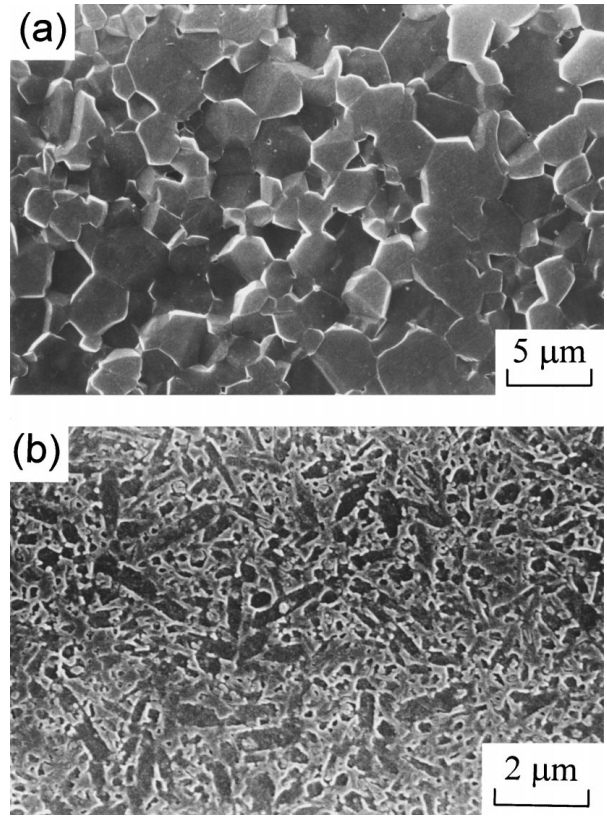

Figure 1 The microstructures of (a) the Al_2O_3 specimen hot-pressed at 1400°C for 1 h in Ar, (b) the Si_3N_4 specimen hot-pressed at 1750°C for 1 h in N_2.

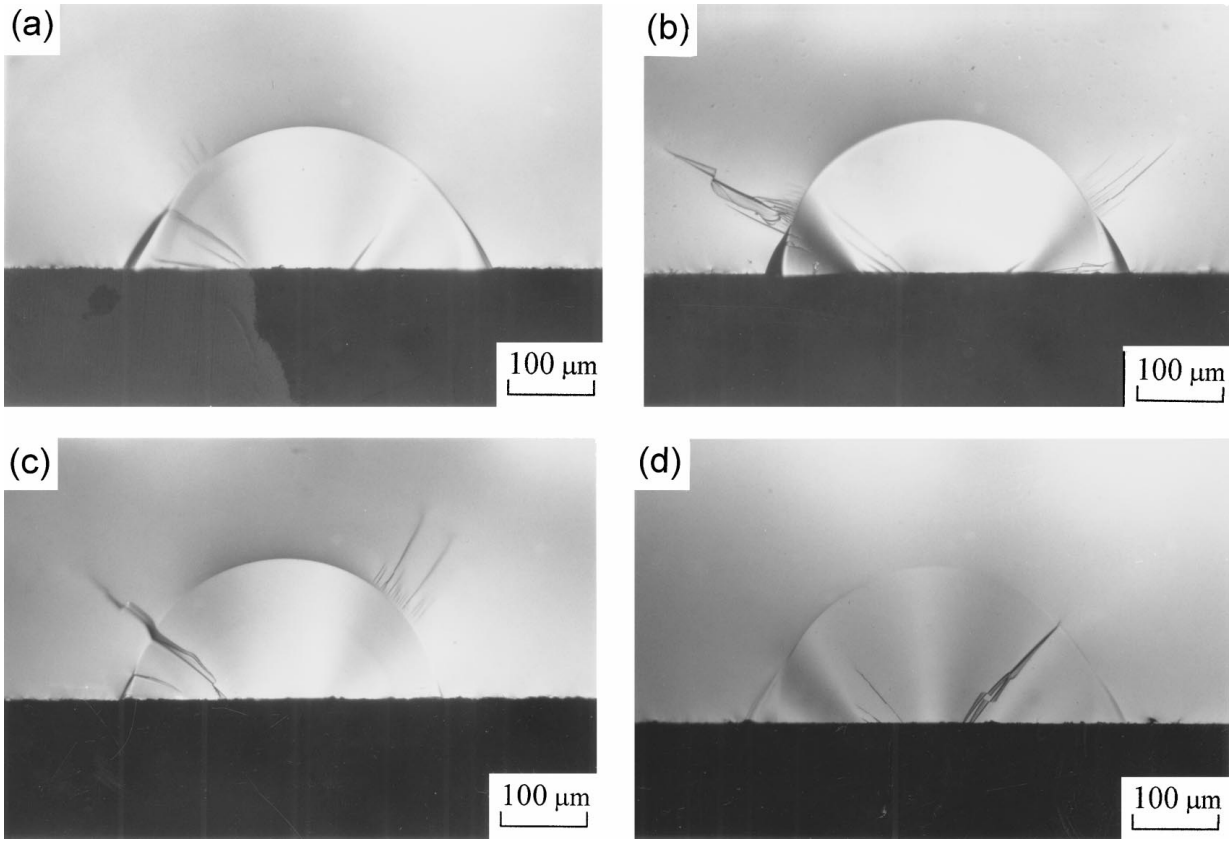

Figure 2 Optical photographs of a Knoop indentation-induced precrack (37 N load) in soda-lime glass specimens which were fractured at the crosshead speed of (a) 0.01 mm/min, (b) 0.05 mm/min, (c) 0.5 mm/min and (d) 5.0 mm/min.

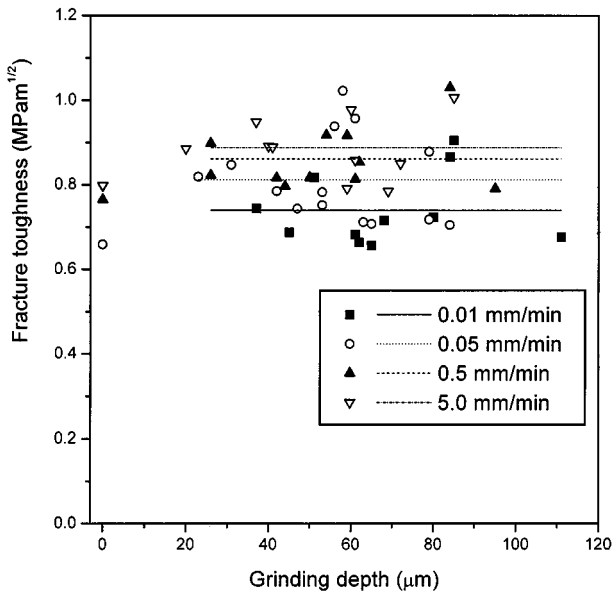

Figure 3 Plot of apparent fracture toughness versus surface grinding depth for soda-lime glass specimens.

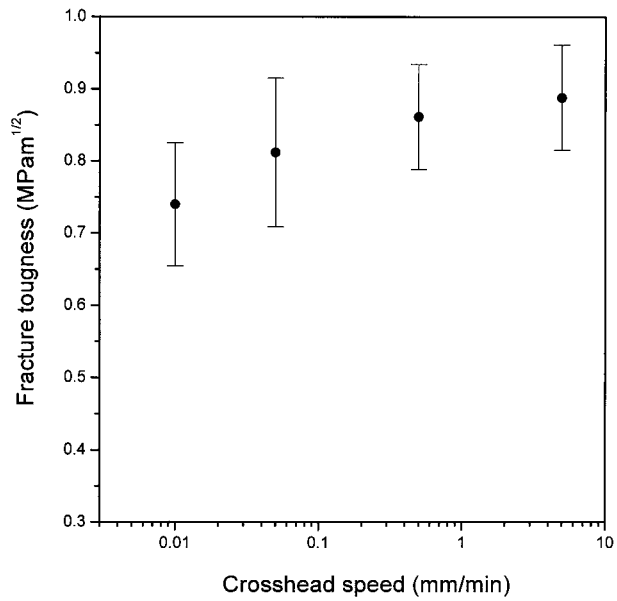

Figure 4 Plot of average fracture toughness versus crosshead speed for soda-lime glass specimens.

are clearly seen, but halo regions around the precracks can not be observed although crack extension must occur during the bending test, because it was reported that soda-lime glass was susceptible to SCG by the stress corrosion cracking [13–15]. The fracture toughness was, therefore, calculated by using the initial precrack size and the flexure strength. Fig. 3 shows the relation between the apparent fracture toughness and grinding depth. At any crosshead speed, the fracture toughness becomes a constant value above a certain grinding depth ($\approx$25 μm) which is almost 2.5 times of the indentation depth. The average fracture toughness in the constant region (grinding depth $>$25 μm) was obtained to be 0.74 ± 0.09 MPam$^{1/2}$, 0.81 ± 0.1 MPam$^{1/2}$, 0.86 ± 0.07 MPam$^{1/2}$ and 0.88 ± 0.07 MPam$^{1/2}$ for the crosshead speed of 0.01 mm/min, 0.05 mm/min, 0.5 mm/min and 5.0 mm/min, respectively. As shown in Fig. 4, the fracture toughness increases with increasing

the crosshead speed, and reached a constant value above a certain crosshead speed (0.5 mm/min). The change in the fracture toughness must be caused by SCG through the degradation in flexure strength of the precracked specimen. However, the critical crack size at fracture was not really observed on the fracture surface of glass specimens. The difficulty in observing the critical crack size at fracture on the fractured surface was reported in glass system [8, 15]. If we could calculate the fracture toughness from the critical crack size at fracture at any crosshead speed, there may have been no dependence of the fracture toughness on the crosshead speed. Practically for measuring the fracture toughness of soda-lime glass by the SCF method, it is better to conduct a bending test under higher crosshead speeds (over 0.5 mm/min) or in an inert environment to eliminate the SCG.

3.2.2. Al_2O_3 specimen

Figs 5 and 6 show the optical photographs of the fractured surfaces of Al_2O_3 specimens which were tilted 0° and ∼0.5° off perpendicular to the Knoop indenter axis during the indentation. Hereafter, the Al_2O_3 specimens tilted 0° and ∼0.5° during indentation are referred to as 0- and 5-specimens, respectively. In this case, contrary to the soda-lime glass specimens, halo regions (relatively dark regions) were observed around initial precracks (relatively bright region inside halo regions). A contrast of the halo regions to other regions was caused by the difference in the fracture mode among the regions. In the halo regions, fracture occurred intergranularly, whereas transgranular fracture occurred in the precrack and fast fracture regions as reported by Quinn *et al*. [9]. Fig. 7 shows the relation between the halo size and the initial precrack size. In both cases of 0-, 5-specimens, the halo size increased as the crosshead speed decreased, and this trend was independent of the initial precrack size.

As shown in Figs 5 and 6, there were two kinds of crack size i.e. initial precrack size and critical crack size at fracture (halo incorporated crack size) on the fractured surface of the Al_2O_3 specimens. At first, we calculated the fracture toughness from the flexure strength and the initial precrack size. Fig. 8a and b show the average fracture toughness (open marks) as a function of the crosshead speed for the 0- and 5-specimens, respectively. In this calculation, the critical grinding depth to remove the residual stress around a Knoop indent was assumed to be 3 h where h is the indentation depth. As can be seen in these figures, the fracture toughness (open marks) was largely dependent on the crosshead speed for both 0- and 5-specimens as in the case of the soda-lime glass specimens. This is because the change in crack size (halo size) during a bending test is not considered in the calculation.

For the reason, the fracture toughness was recalculated by using the critical crack size at fracture (halo incorporated crack size). Fig. 9 shows the fracture toughness of the Al_2O_3 specimen as a function of the grinding depth. It can be seen from this figure that the fracture toughness increases with increasing the grinding depth and reaches a constant value above a certain grinding depth (≈20 μm). The critical depth in this specimen corresponds to the 3 h, where h is the indentation depth. In the constant regions, the average fracture toughness for the 0-specimen was obtained as 3.99 ± 0.09 MPam$^{1/2}$, 3.96 ± 0.09 MPam$^{1/2}$ and 3.87 ± 0.06 MPam$^{1/2}$ for the crosshead speed of 0.05 mm/min, 0.5 mm/min and 2.0 mm/min, respectively. For the 5-specimens, these values were 4.02 ± 0.11 MPam$^{1/2}$, 3.99 ± 0.09 MPam$^{1/2}$ and 4.00 ± 0.06 MPam$^{1/2}$ for the crosshead speed of 0.05 mm/min, 0.5 mm/min and 2.0 mm/min, respectively. The relations between the fracture toughness and the crosshead speed for the 0- and 5-specimens were also plotted in Fig. 8a and b as closed marks, respectively. As can be seen in these figures, the fracture toughness calculated

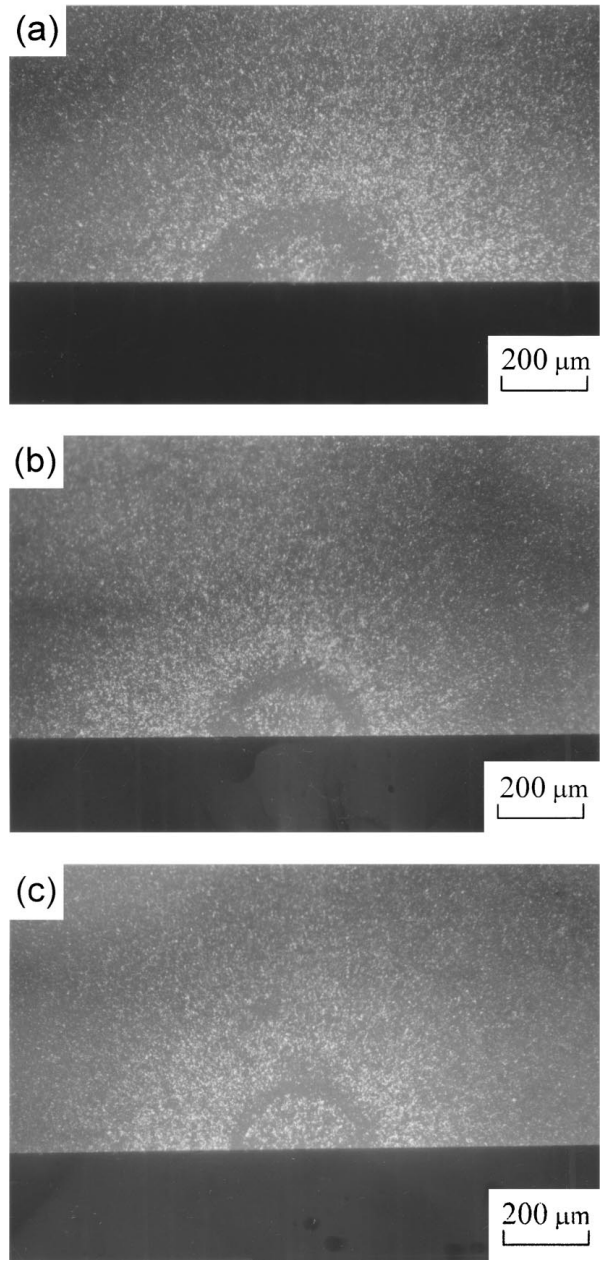

Figure 5 Optical photographs of a Knoop indentation-induced precrack (49 N load) in Al_2O_3 specimens which were fractured at the crosshead speed of (a) 0.05 mm/min, (b) 0.5 mm/min and (c) 2.0 mm/min. The Al_2O_3 specimens were not tilted off perpendicular to the diamond indenter axis during the indentation.

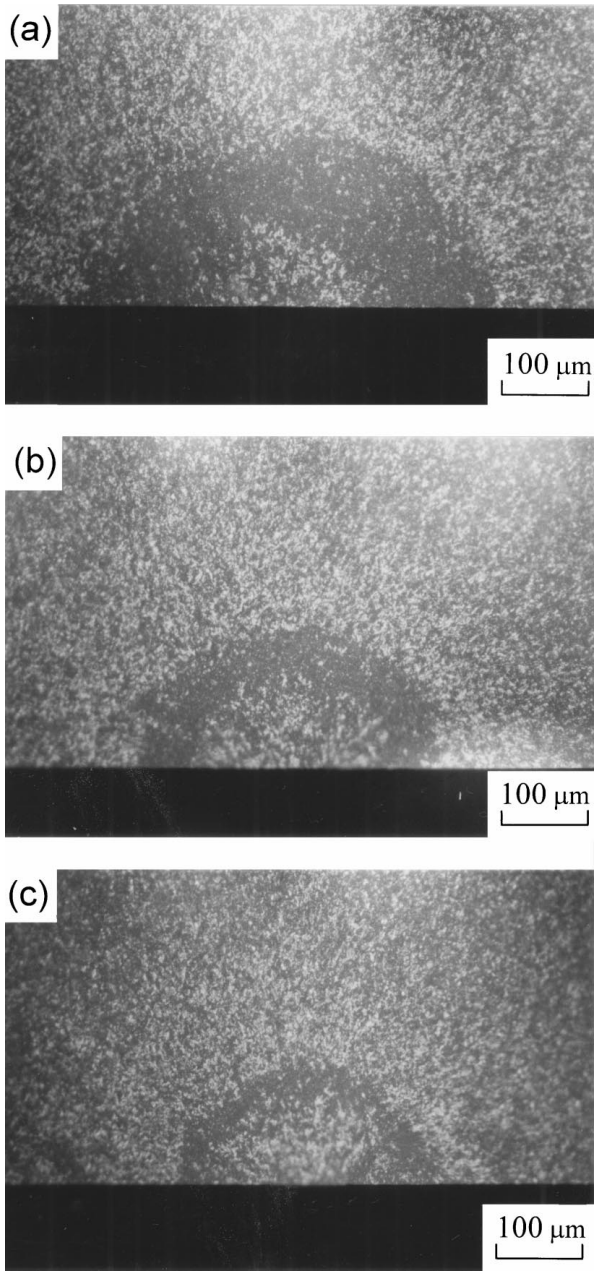

Figure 6 Optical photographs of a Knoop indentation-induced precrack (49 N load) in Al_2O_3 specimens which were fractured at the crosshead speed of (a) 0.05 mm/min, (b) 0.5 mm/min and (c) 2.0 mm/min. The Al_2O_3 specimens were tilted ~0.5° off perpendicular to the diamond indenter axis during the indentation.

from the critical crack size at fracture does not depend on the crosshead speed, and there is no difference in the values between 0- and 5-specimens. It means that the change in the crosshead speed and tilting a specimen do not cause any systematic error in the measurement of fracture toughness of Al_2O_3 specimens.

Quinn *et al*. has reported that the fracture toughness of Al_2O_3 was to be more reasonable by incorporation of the halo into the crack size [9]. In this study, it is newly shown that the fracture toughness is also independent of the crosshead speed when the critical crack size (halo incorporated crack size) at fracture is used for the calculation. This is because the increase in crack size during loading is counterbalanced by the resultant decrease in the flexure strength as shown in Equation 1.

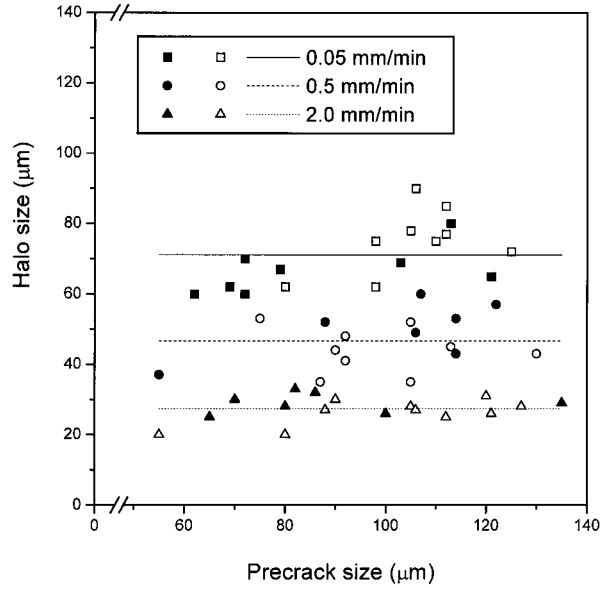

Figure 7 Plot of halo size (a) versus precrack size (a) for Al_2O_3 specimens; closed and open marks are for the 0-specimens and 5-specimens, respectively.

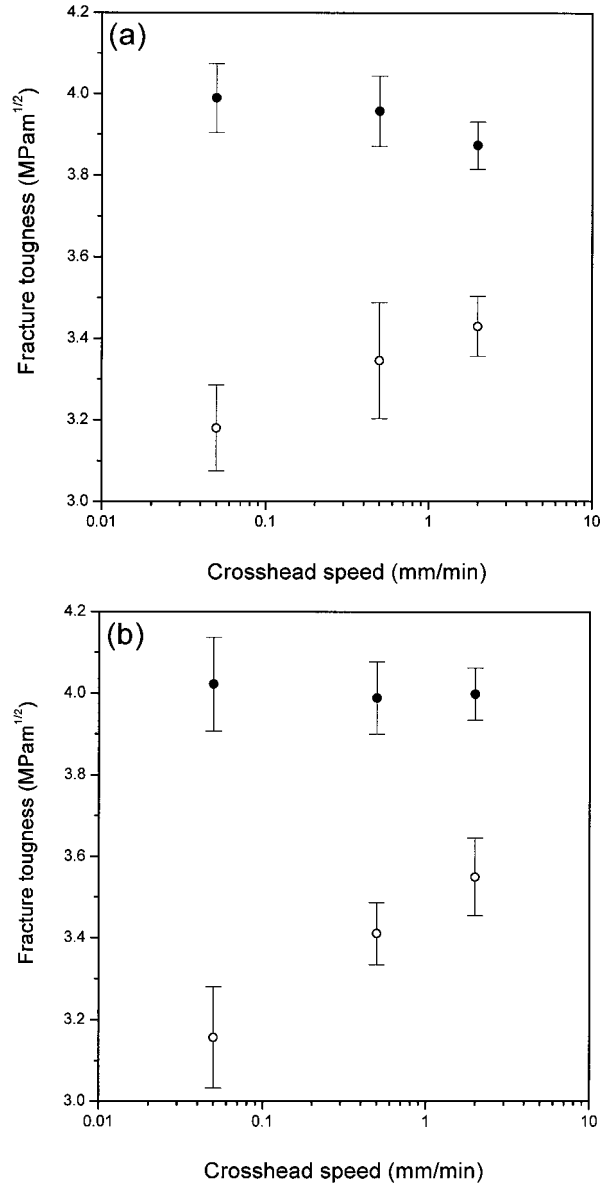

Figure 8 Plot of average fracture toughness versus crosshead speed for Al_2O_3; (a) 0-specimens, (b) 5-specimens. Closed and open marks are for the values calculated by the crack size *with* and *without* halo, respectively.

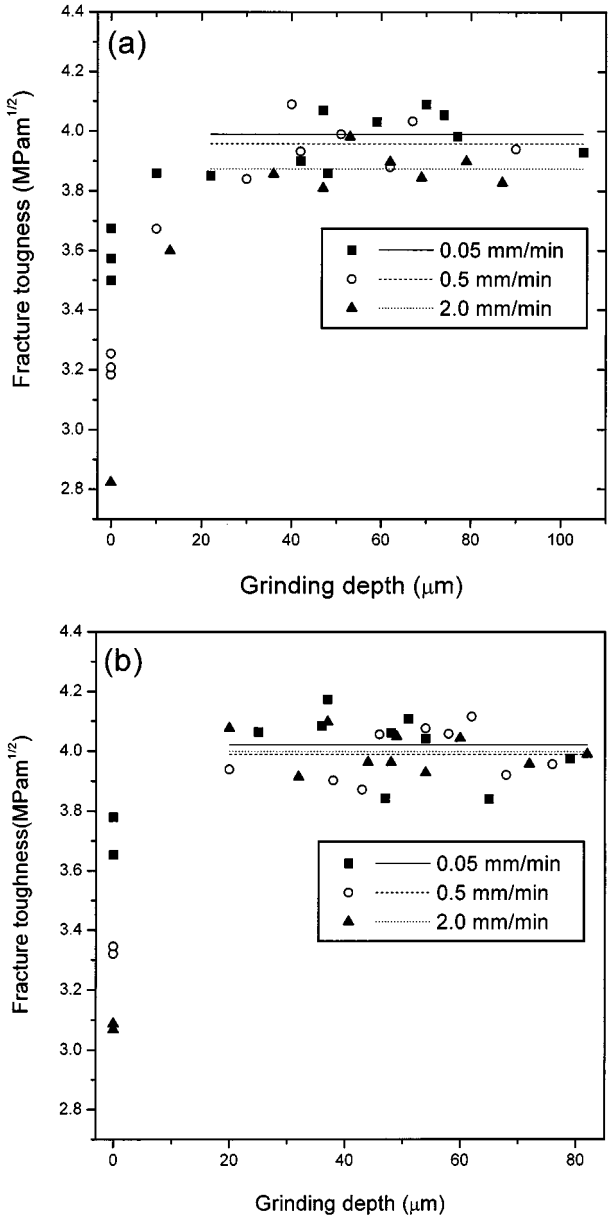

Figure 9 Plot of apparent fracture toughness versus surface grinding depth for Al_2O_3; (a) 0-specimens, (b) 5-specimens.

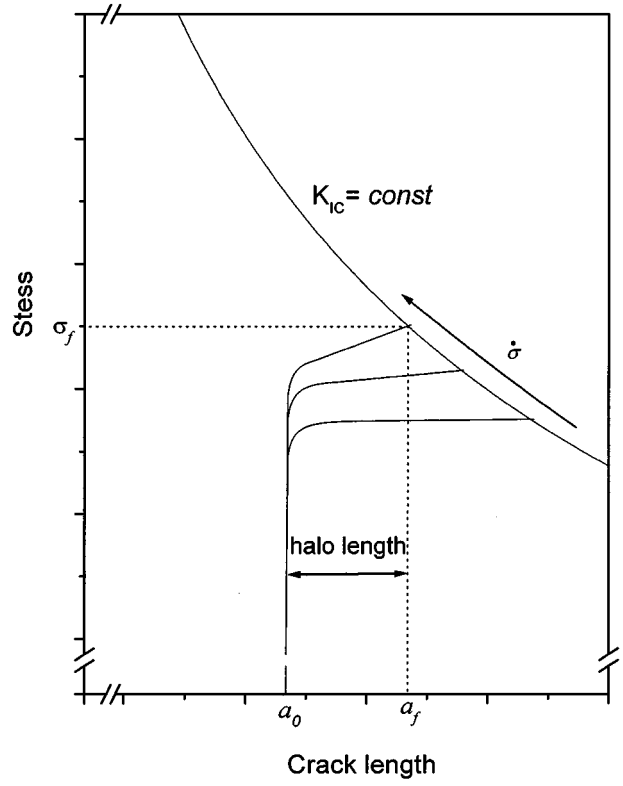

Figure 10 Schematic illustration of the relation between crack size (halo size) and fracture strength for the case of Al_2O_3 where SCG occurs.

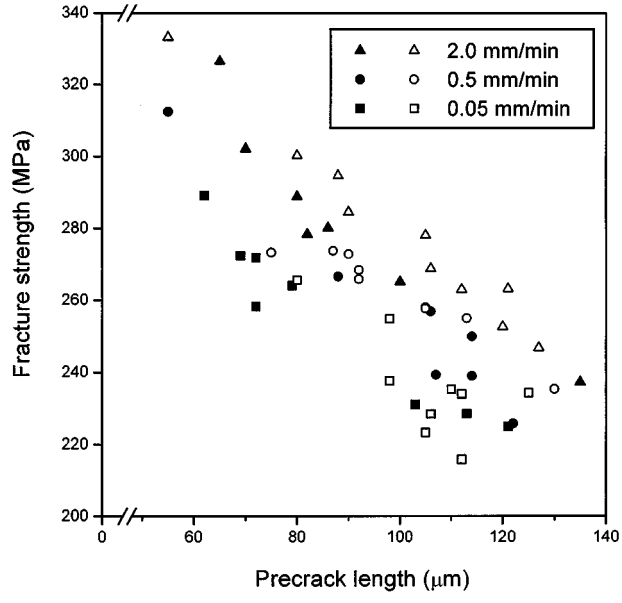

Figure 11 Plot of flexure strength versus initial precrack size for Al_2O_3 specimens; closed and open marks are for the 0-specimens and 5-specimens, respectively.

For most of ceramic and glass materials, a subcritical crack growth rate can be expressed as a following equation:

$$V = AK_I^n \tag{2}$$

where K_I is the stress intensity factor, A and n are constants that depend on the environment and the material. On substituting Equation 1 into Equation 2, the following equation can be obtained.

$$a^{-\frac{n}{2}} da = AY^n \sigma^n \, dt \tag{3}$$

In the case of constant stress rate ($\sigma = \dot{\sigma} t$), integration of the Equation 3 yields the following equation:

$$\sigma = \left\{ \frac{2(n+1)\dot{\sigma}}{AY^n(n-2)} \left[\left(\frac{1}{a_0}\right)^{\frac{n}{2}-1} - \left(\frac{1}{a}\right)^{\frac{n}{2}-1} \right] \right\}^{\frac{1}{(n+1)}} \tag{4}$$

where a_0 is the initial crack size which is determined by the indentation load and grinding depth. The average value of stress rate ($\dot{\sigma}$) is proportional to the crosshead speed. By substituting the reported data of Pletka *et al.* [16] into the Equation 4, the flexure strength of a precracked specimen can be obtained as shown in Fig. 10, when the initial precrack size and stress rate are arbitrary given. In this figure, we consider two regions in which the rate of the reaction at a crack tip controls crack extension and the diffusion of corrosive species to the crack tip controls crack extension. Although the constants used to represent this figure do

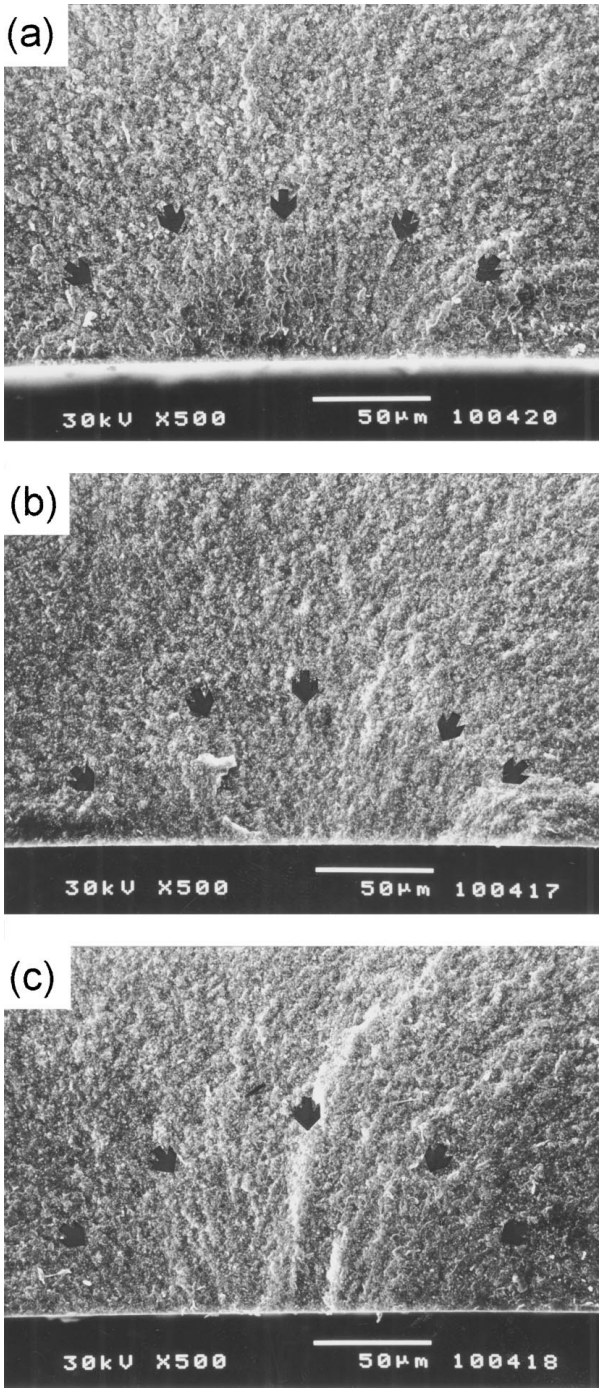

Figure 12 SEM photographs of a Knoop indentation-induced precrack (49 N load) in Si_3N_4 specimens which were fractured at the crosshead speed of (a) 0.05 mm/min, (b) 0.5 mm/min, and (c) 5.0 mm/min. Arrows outline precracks.

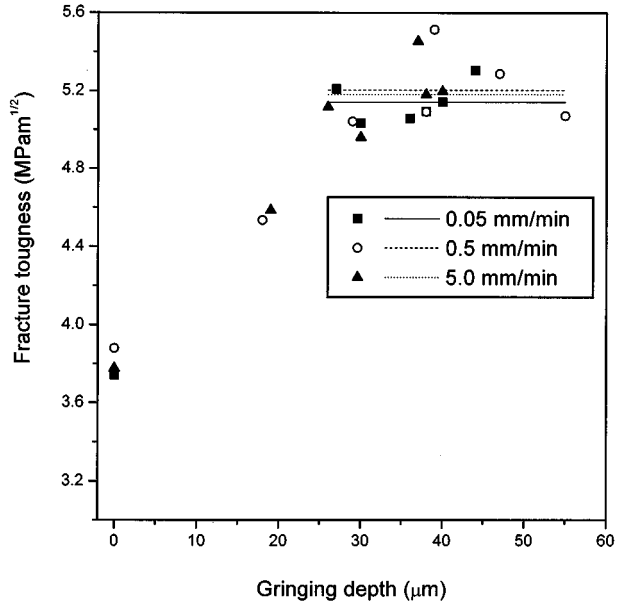

Figure 13 Plot of apparent fracture toughness versus surface grinding depth for Si_3N_4 specimens.

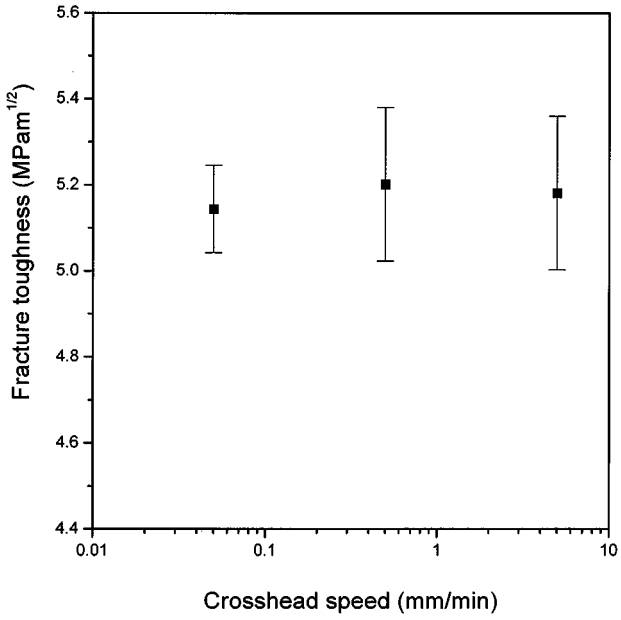

Figure 14 Plot of average fracture toughness versus crosshead speed for Si_3N_4 specimens.

not correctly correspond to our result, the qualitative explanation is possible. As can be seen in Fig. 10, for the same initial crack size, the halo size ($a_f - a_0$) increases as the crosshead speed decreases, and this trend coincides with the result obtained in this study as shown in Fig. 7. Furthermore, the flexure strength increases with increasing crosshead speed under the constant fracture toughness condition. The relation between fracture strength and the initial precrack size for 0-, 5-specimens was shown in Fig. 11. From this figure, the strength of the Al_2O_3 specimen was confirmed to increase with the increase in the crosshead speed at every initial precrack size. The constant fracture toughness with the crosshead speed is, therefore, thought to be caused by the fact that the increased halo size is offset by the decreased fracture strength.

From these results, if the halo region appears by the SCG during the loading as shown in the Al_2O_3 specimens, the critical crack size (i.e. the crack size incorporated with halo) must be used to calculate the fracture toughness because the obtained fracture toughness does not depend on the crosshead speed, and thus becomes a material constant. Namely, in such a case, the crosshead speed is not important for measuring the fracture toughness at least from 0.05 mm/min to 2.0 mm/min.

3.2.3. Si_3N_4 specimen

Fig. 12 shows the SEM photographs of the fractured surfaces of the Si_3N_4 specimen. Contrary to the Al_2O_3

specimen, halo regions could not be observed around periphery of the initial precrack at any crosshead speed. It has been reported that the SCG in Si_3N_4 mainly appeared at high temperatures [17]. In NC-132 Si_3N_4, a halo region was reported to appear even at room temperature, but the halo was thought to be due to the precrack tilt, not SCG [8]. In this study, the halo region induced by SCG did not appear in the Si_3N_4 specimens tested at room temperature. It means that the critical crack size at fracture is equal to the initial precrack size induced by indentation, and this value must be used for fracture toughness calculation, unlike the soda-lime specimen mentioned above.

Fig. 13 shows the fracture toughness of the Si_3N_4 specimen as a function of grinding depth. The fracture toughness increases with increasing the grinding depth and reaches a constant value ($\approx$25 μm). This critical depth corresponds to the 3.5 h, where h is the indentation depth. The average fracture toughness of the Si_3N_4 specimens above the critical grinding depth was calculated to be 5.14 ± 0.10 MPam$^{1/2}$, 5.20 ± 0.18 MPam$^{1/2}$ and 5.18 ± 0.18 MPam$^{1/2}$ for the crosshead speed of 0.05 mm/min, 0.5 mm/min and 5.0 mm/min, respectively. These data were plotted against the crosshead speed in Fig. 14. Although the halo region could not be observed as in the case of soda-lime glass specimens, the fracture toughness of the Si_3N_4 specimens calculated from the initial precrack size was almost independent of the crosshead speed. This is because the SCG and plastic yielding do not occur at room temperature in the Si_3N_4 specimens as has been reported by Lange [18], even though the impurity levels in the Si_3N_4 powders are different from each other.

4. Conclusion

The fracture toughness of the Al_2O_3 and Si_3N_4 specimens determined by SCF method was independent of the crosshead speed, although the appearance of halo region was quite different. In the Al_2O_3 specimens, the increase in crack size caused by SCG was counterbalanced by the decrease in the flexure strength, and thus the fracture toughness was relatively constant irrespective of the crosshead speed. The fracture toughness of the Si_3N_4 specimens was also independent of the crosshead speed, because the initial precrack size was equal to the critical crack size at fracture. In soda-lime glass specimens, halo region could not be observed. The fracture toughness was, however, dependent on the crosshead speed unlike the Si_3N_4 specimens. This is probably due to the difficulty in determining the critical crack size at fracture. For glass, it is recommended that a bending test be performed under relatively higher crosshead speed (over 0.5 mm/min) or in an inert environment.

Acknowledgements

J.-K. Park would like to thank the Korean Organization of Science and Engineering Foundation (KOSEF) for their financial support through the Center for Interface Science and Engineering of Materials (CISEM).

References

1. P. KENNY, *Powder Met.* **14** (1971) 22.
2. K. R. KINSMAN, in "Deformation of Ceramic Materials," edited by R. C. Bradt and R. E. Tressler (Plenum Press, New York, 1975) p. 465.
3. J. J. PETROVIC, L. A. JACOBSON, P. A. TALTY and A. K. VASUDEVAN, *J. Amer. Ceram. Soc.* **58** (1975) 113.
4. J. J. PETROVIC, R. A. DIRKS, L. A. JACOBSON and M. G. MENDIRATTA, *ibid.* **59** (1976) 177.
5. J. C. NEWMAN. JR., I. S. RAJU, *Eng. Fract. Mech.* **15** (1981) 185.
6. C. A. TRACY and G. D. QUINN, *Ceram. Eng. Sci. Proc.* **15** (1994) 837.
7. G. D. QUINN, R. J. GETTINGS and J. J. KÜBLER, *ibid.* **15** (1994) 846.
8. *Idem.*, in "Ceramic Transactions," Vol. 64, edited by J. R. Varner, V. D. Frechette and G. D. Quinn (American Ceramic Society, Westerville, OH, 1996) p. 107.
9. J. J. SWAB and G. D. QUINN, *J. Amer. Ceram. Soc.* **81** (1998) 2261.
10. ISO/TC 206/SC, N209, New Work Item Proposal (1998).
11. G. D. QUINN, J. J. KÜBLER and R. J. GETTINGS, in "VAMAS Technical Report" (National Institute of Standards and Technology, Gaithersburg, MD, June, 1994) #17.
12. ASTM C 1161, "Annual Book of ASTM Standards," Vol. 15.01 (ASTM, West Conshohoken, PA., 1997) p. 324.
13. S. M. WIEDERHORN and L. H. BOLTZ, *J. Amer. Ceram. Soc.* **53** (1970) 543.
14. A. G. EVANS, *Int. J. Fract.* **10** (1974) 251.
15. J. J. MECHOLSKY, A. C. GONZALEZ and S. W. FREIMAN, *J. Amer. Ceram. Soc.* **62** (1979) 577.
16. B. J. PLETKA and S. M. WIEDERHORN, *J. Mater. Sci.* **17** (1982) 1257.
17. R. K. GOVILA, *J. Amer. Ceram. Soc.* **63** (1980) 319.
18. F. F. LANGE, *ibid.* **57** (1974) 84.

Received 7 December 1999
and accepted 31 July 2000